Angewandte Chemie
Eine Zeitschrift der Gesellschaft Deutscher Chemiker

Supporting Information

69451 Weinheim, Germany

Facile and Scalable Preparation of Pure and Dense DNA Origami Solutions**

*Evi Stahl, Thomas G. Martin, Florian Praetorius, and Hendrik Dietz**

anie_201405991_sm_miscellaneous_information.pdf

Guide to the supporting information

Note S1: Schematic illustration of the PEG purification cycle

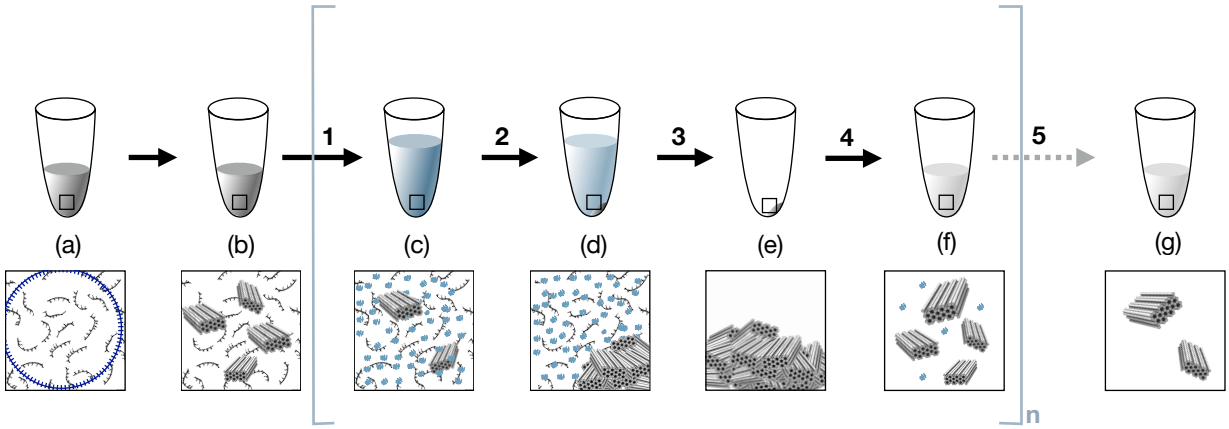

Scheme S1. Step-by-step guide of PEG purification procedure for DNA objects (b, exemplary object depicted as 42-helix bundle), self-assembled from a stochiometric mixture of a long circular single-stranded template molecule (a, dark blue circle) with several hundreds of short oligonucleotides as staple molecules in excess (a, b black dashed lines). **1)** To purify DNA objects from non-integrated excess staple-strands, add one volume of precipitation buffer to an unpurified sample (b) and mix thoroughly to obtain a homogeneous distribution of assembly-products and buffer components, especially PEG 8000 (c, light blue). **2)** Pellet precipitated DNA objects by centrifugation. **3)** Remove the supernatant in (d). **4)** Dissolve the obtained pellet (e) in target buffer and incubate the purified sample (f) overnight at RT prior to use. If desired, enter another cycle for further purification, buffer exchange, or increase in concentration. **5)** For complete removal of residual PEG (g) spin the sample using MWCO filter devices (max. three times). Depending on the type of downstream application, the sample can be inserted as pellet (e), re-dissolved in target buffer (f) or completely free from PEG (g) into following experiments.

Note S2: Detailed methods

Image processing:

For class averages shown in Figure 3 and S8, libraries of individual particle micrographs were created by particle picking using the EMAN2 boxing routine (Tang, Peng et al. 2007). Generation of average particle micrographs was performed with approximately 800 particle micrographs (Figure 3) or approx. 300 particle micrographs (Figure S8) per sample using Xmipp mlf2d algorithm (Scheres, Nunez-Ramirez et al. 2008).

De-Bruijn probes:

Analysis of unpaired DNA remainders was carried out using de-Bruiin defect probe oligonucleotides of order three as described previously (Wagenbauer, Wachauf et al. 2014). The probe molecules were labeled with cyanine-5 dyes (instead of cyanine-3 dyes as in the study by Wagenbauer et al).

Absorption spectroscopy:

UV-Vis detection was performed in triplicate measurements using a nanophotometer (Implen, Munich, Germany). The samples from Figure 3 were diluted 200-fold and equilibrated overnight.

Detailed experiment description:

Figure 1: The self-assembly products were subjected to one cycle of PEG purification. The obtained pellets were dissolved in the starting volume using a buffer containing 5 mM TRIS, 1 mM EDTA, 5 mM $MgCl_2$ and 5 mM NaCl (pH 8) and equilibrated overnight at RT or 30 °C.

Figure 2/S7: All experiments were carried out in triplicates using a 42-helix bundle object with honeycomb-type lattice packing as a test sample. For **Fig. 2a-c**, 200 µl of the reaction mixture were diluted four-fold in "default buffer" (5 mM TRIS, 1 mM EDTA, 20 mM $MgCl_2$ and 5 mM NaCl (pH 8)) to obtain a starting volume of 800 µl that was mixed 1:1 with "precipitation buffer" (15 % PEG 8000 (w/v), 5 mM Tris, 1 mM EDTA and 505 mM NaCl). After centrifugation, the pelleted materials were dissolved in the previous volume to re-establish the initial volume of the sample before adding precipitation buffer. The solutions were equilibrated for approx. 30 min. Then, a 20 µl sample was extracted for later analysis. The next cycle of PEG purification was carried out accordingly with 780 µl volume of sample and PEG precipitation buffer. In total, ten cycles of PEG purification were performed in this fashion, extracting a 20 µl sample at every round. For **Fig. 2d-f**, we subjected 50 µl of the reaction mixture to AGE extraction and to one and five rounds of PEG purification and molecular-weight cut-off filtration, respectively. Purified samples were dissolved in the volume of the starting sample. Filtration was performed using Amicon Ultra-0.5 (Millipore) centrifugal filter devices with a 100 kDa molecular weight cutoff-membrane. 50 µl sample was mixed with 450 µl default buffer and centrifuged at 2,000 g for 30 min. For additional purification cycles, the reaction vessel was filled with 480 µl default buffer and centrifuged again. Sample

recovery was achieved by spinning the inverted filter device for 10 min at 1,000 g. The sample volume after spinning was adjusted to the volume of the starting sample. AGE-purification was performed after electrophoretic separation of the reaction mixture in a 1.5 % agarose-gel matrix, followed by excision of the leading band. For physical extraction, the gel slices were transferred to Freeze 'N Squeeze filter spin columns (BioRad) and spun at 10,000 g for 10 min. Due to three-fold volume increase after AGE-purification, all samples were diluted to 150 µl for comparative analysis. The experiments illustrated in **Fig. 2g-i** were carried out with a PEG precipitation buffer containing a mixture of 13.5 % PEG 8000 (w/v) and 1.5 % PEG 8000 di-fluorescein (w/v) (Chemicell, Berlin). Residual liquid retained at the pellet by surface tension was removed with a thin stripe of filter paper without touching the pellet (Whatman). The obtained pellets were re-dissolved in default buffer at the same volume as the starting sample. The experiments shown in **Fig. S7** were carried with a PEG precipitation buffer containing a mixture of 12 % PEG 8000 (w/v) and 3 % PEG 8000 di-fluorescein (w/v) (Chemicell, Berlin). Residual liquid retained at the pellet by surface tension was removed with a thin stripe of filter paper without touching the pellet (Whatman). The obtained pellets were re-dissolved in default buffer at the same volume as the starting sample. The purified sample was washed using Amicon Ultra-0.5 (Millipore) centrifugal filter devices with a 10k Da, 30k Da, or 100 kDa molecular weight cut-off membrane as described above. The sample volume after spinning was adjusted to the volume of the starting sample.

Figure 3/S8: The set of experiments depicted in Figure 3 and Figure S8 was performed with reaction mixtures containing a variant of Rothemund's Rectangle (RR), a 24-helix bundle and 42-helix bundle, respectively. PEG purification was performed with all samples in a 50 ml Falcon tube that was centrifuged for 40 min at 16,000 g using a bench top centrifuge with a fixed angle rotor (Hettich Rotanta 460R, Stuttgart, Germany). The obtained pellet of the sample containing the 24–helix bundle and the RR were dissolved in 1 ml and transferred to a 2 ml reaction tube to carry out a second pelleting cycle. The sample containing 42-helix bundle was subjected to a single cycle of PEG treatment. The obtained pellets were dried overnight at room temperature, followed by 3 h vacuum spinning at 40 °C to achieve complete drying of the pellet.

Note S3: Parameter screen for optimizing PEG purification

Screen for optimal PEG 8000 concentration

To test the influence of PEG-concentration on purification efficiency, we subjected a reaction mixture containing the multi-layer DNA origami object in square lattice design called “pointer” from Bai et al 2012 (reference 2h in main text) to two cycles of PEG purification at various PEG-contents while keeping the content of mono- and divalents salts constant. A final concentration of 7.5 % PEG 8000 (w/v) gave best results with respect to sample recovery and separation efficiency. Lower concentrations of PEG resulted in loss of monomers in the supernatant (Figure S1a), while a higher PEG concentration induced undesired co-precipitation of non-integrated staple strands (Figure S1b).

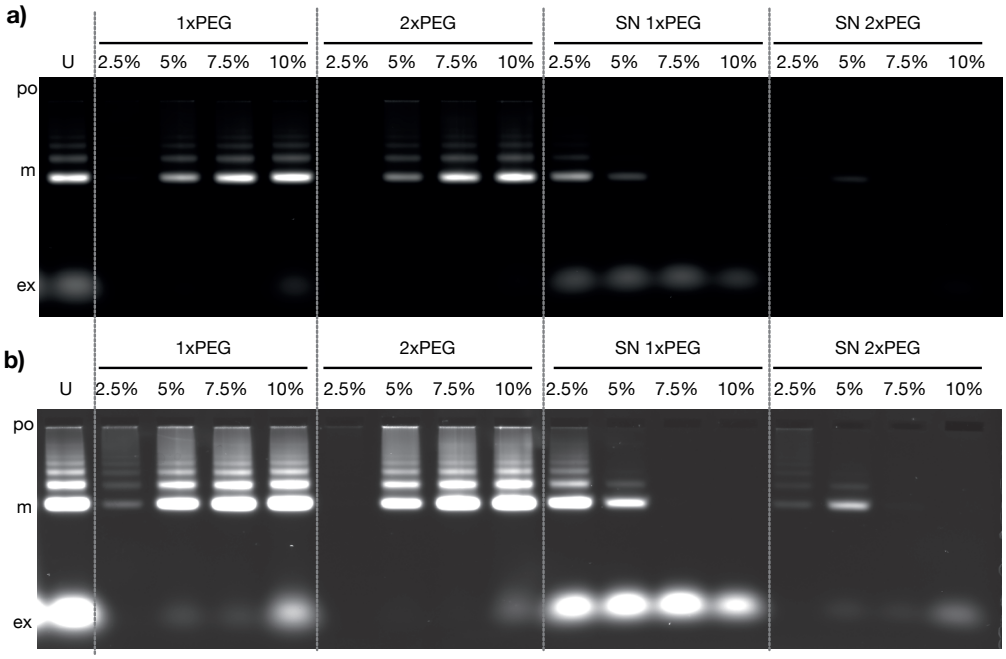

Figure S1. Concentration screen for PEG 8000. Gel electrophoretic analysis of attempts to pellet a multi-layer DNA origami object in square-lattice packing (see ref 2h, main text) using various concentrations of PEG 8000 and a constant salt concentration of 255 mM NaCl and 10 mM $MgCl_2$ in the 1:1 mixture of PEG-solution and sample. The samples were re-dissolved in default buffer. a) laser-scanned agarose gel image, auto-leveled; b) contrast-enhanced version of (a) to visualize content of co-precipitated staples. Labels: U: unpurified reaction mixture; 1xPEG: once-precipitated sample; 2xPEG: twice-precipitated sample; SN: supernatant.

Chain length of the crowding agent

Our work builds on previously published protocols for PEG precipitation of plasmids, phages and phage-like DNA objects, where PEG molecules with an average molecular weight of 8000 Da (denoted as PEG 8000) were used as crowding agent. (Sambrook et al. 2001; Stein et al. 2009; Bellot et al. 2013). We found that PEG 8000 is generally well suited for purification of DNA origami objects (Figure 1), but we also explored the influence of the molecular weight of PEG on the precipitation success using different types of PEG with molecular weights ranging from 400 to 20,000 Dalton. To this end, we prepared precipitation buffers containing various types of PEG molecules at a concentration of 15 % (w/v) and mixed them 1 to 1 with a reaction mixture of the 42-helix bundle to achieve a final concentration of 7.5 % (w/v) PEG, 5 mM Tris, 255 mM NaCl and 10 mM $MgCl_2$. Gel-electrophoretic analysis of the re-dissolved pellets and their corresponding supernatants revealed that PEG 6000, 8000, and 10,000 are best suited for purification of DNA objects. Lower PEG chain lengths resulted in reduced sample recovery, as shown by the presence of folded DNA objects in the supernatant (Figure S2a, lower row).

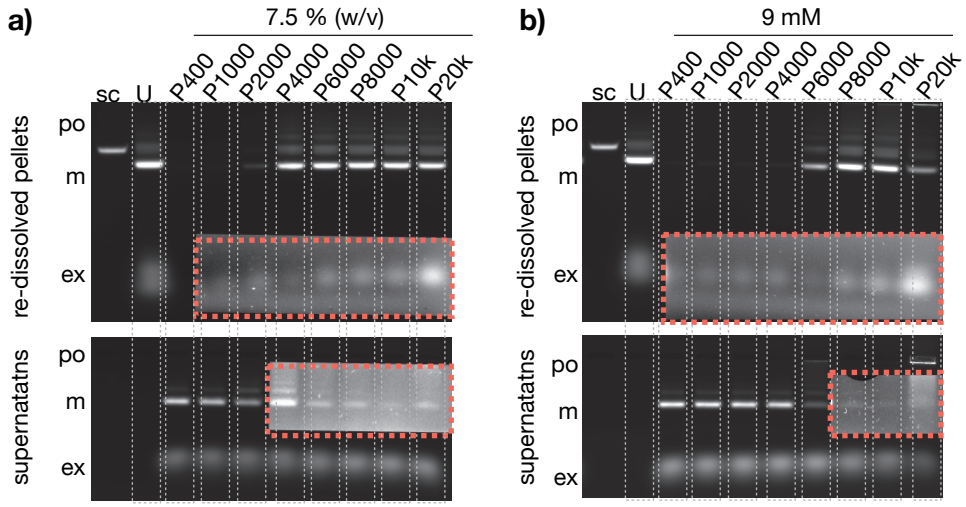

Figure S2. Gel-electrophoretic analysis of the influence of the chain length of PEG used for purification of a 42-helix bundle reaction mixture. a) Image of a gel where DNA objects were precipitated with different PEG-types each at a final concentration of 7.5 % (w/v) PEG, 255 mM NaCl, 5 mM Tris and 10 mM $MgCl_2$. b) as in (a), but at a final concentration of 9 mM for each PEG-type. Upper row: re-dissolved pellets; lower row: corresponding supernatants. Labels: U: unpurified reaction mixture; po: gel pocket; m: folded monomers; ex: non-integrated staple strands. Boxed areas were enhanced in brightness to reveal faint bands.

Purification of DNA objects using PEG 20,000 resulted in increased co-precipitation of non-integrated staple strands (Figure S2a, upper row). Moreover, solutions containing PEG 20,000 at a concentration of 15 % (w/v) were more viscous compared to shorter PEG-chain lengths and thus

harder to handle. Our results suggest that the decrease in depletion efficiency when using shorter crowding polymers can be compensated by using a higher concentration of those molecules. At a concentration of 9 mM PEG, however, PEG 8000 is best suited for purification of DNA objects from non-integrated staple strands (Figure S2b). Gel-electrophoretic analysis of purified samples and their corresponding supernatants showed that the use of lower-molecular weight PEG resulted in insufficient sample recovery, while already PEG 10,000 resulted in co-precipitation of staple molecules. A final concentration of 9 mM PEG 20,000 lead to sample aggregation and poor separation efficiency (Figure S2b). Our results are in accordance with earlier studies on the effect of PEG chain length for virus precipitation, which found that PEG 1500 or lower is less efficient in particle precipitation compared to PEG 6000-7500 (Yamamoto et al. 1970; Zimmerman & Minton 1993, Vajda et al 1978). As well, other studies for PEG precipitation of double-stranded DNA indicated a lower depletion efficiency for PEG 20,000 compared to PEG 6000 (Humphreys et al. 1975). All other experiments in our study were performed using PEG 8000 (ph.Eur., Carl-Roth).

Screen for optimal spinning time and temperature

We tested the influence of speed and duration of centrifugation when precipitating a reaction mixture of a 42-helix bundle using PEG 8000. Complete sample recovery could be reached at various combinations of these two parameters. Satisfying recovery is obtained at ≥10,000 g acceleration force and ≥15 min spinning time (Fig. S3a-d). Neither speed nor duration of centrifugation showed impact on the co-precipitation of non-integrated staple oligonucleotides. However, we found that the temperature of the 1:1 mixture during the spinning procedure is a critical parameter for separation efficiency. This is indicated by a higher fraction of residual staple strands in samples that were pelleted at 4°C. We attribute this effect to weak interactions of non-integrated oligonucleotides with folded particles (for example at single-stranded loci), which are increased at lower temperatures.

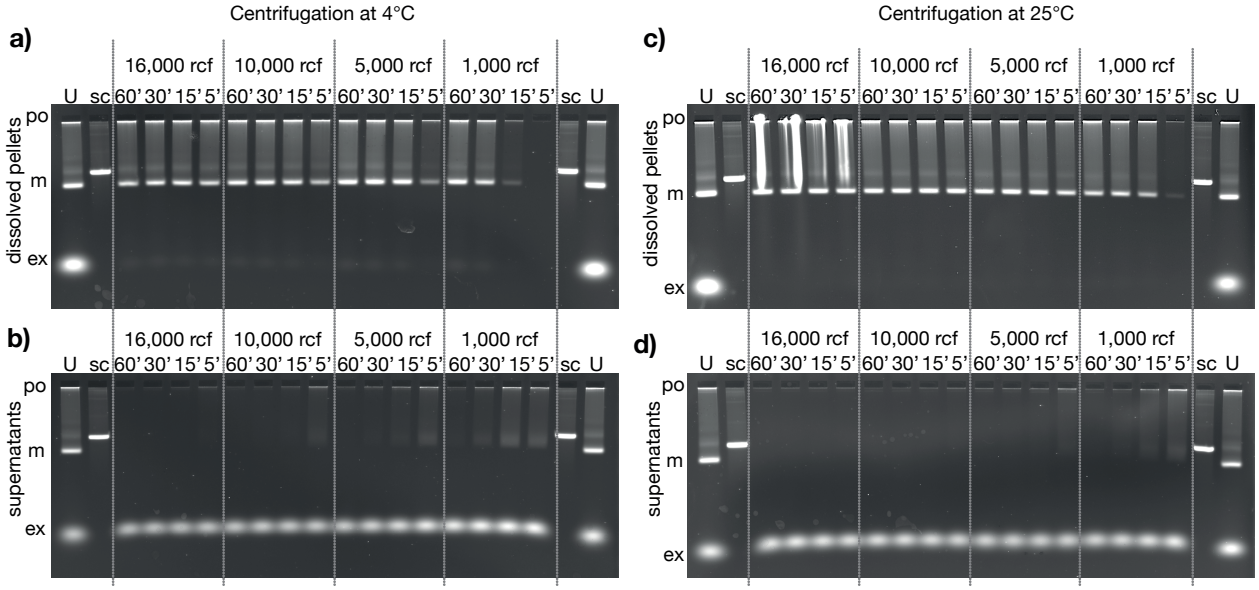

Figure S3. Screen of speed, duration and temperature sensitivity during centrifugation of a reaction mixture of the 42-helix bundle. **a, c)** Image of gels showing gel electrophoretic analysis of dissolved pellets. **b, d)** Corresponding supernatants to samples in (a, c). The screen was performed at 4 °C (a, b) and at RT (c, d). Incomplete recovery is indicated by remaining monomers in the supernatant sample (b, d). Labels: U: unpurified reaction mixture; sc: scaffold strands only; numbers: time of the spinning step in minutes; po*:* gel pocket; m: monomer band of folded particles; ex: non-integrated staple strands.

Presence of cation-types and incubation time with precipitation buffer

A screen of a 42-helix bundle sample PEG purified in the presence of either exclusively sodium chloride or exclusively magnesium chloride suggests that PEG purification can be performed in magnesium free solutions containing only monovalent cations such such conditions are required, but the precipitation does work better when using a mixture of both ion types. A higher fraction of aggregates in the PEG purified samples when using either only sodium chloride or only magnesium chloride in the folding and precipitation buffers indicates lower purification efficiency in both cases (FigS4a and c,d). The presence of only magnesium ions in reaction mixture and precipitation buffer resulted in increased co-precipitation of non-integrated staple strands (Figure S4b). The time of incubation of the mixture of target sample (42-helix bundle) and default precipitation buffer at room temperature did not impact the recovery yield of PEG purification within the times that we tested (1 minute up to 24 hours of incubation, Figure S4f). By contrast, incubation of the sample mixed with PEG solution on ice resulted in co-precipitation of staple-oligonucleotides that increased with the longer incubation times (Figure S4e).

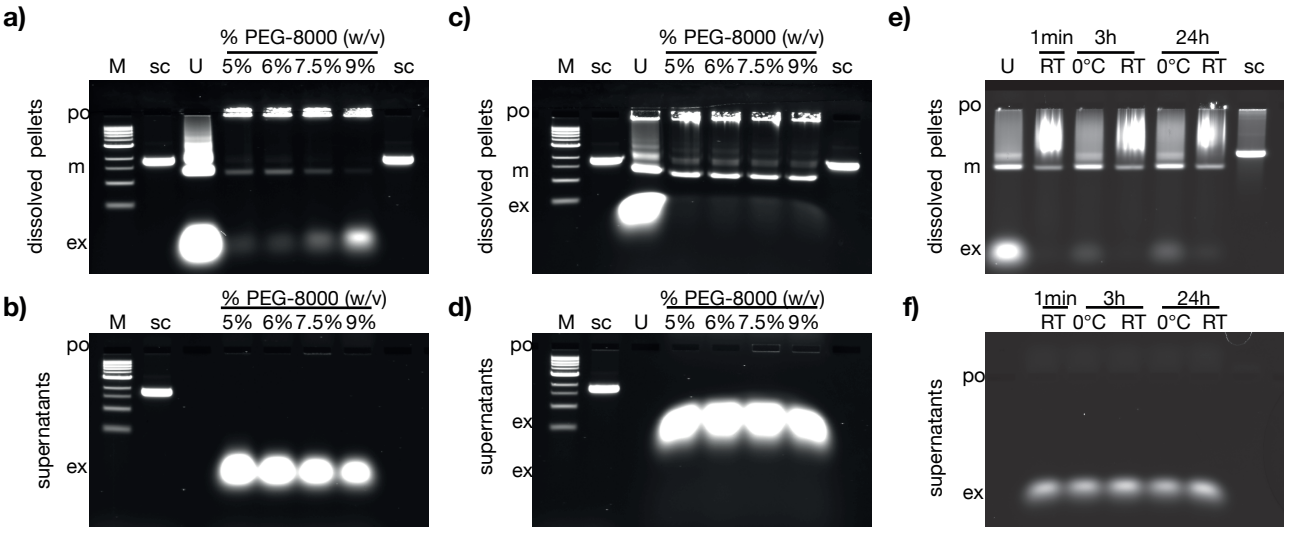

Figure S4. PEG purification in presence of only one type of cations and relevance of incubation time before the spinning step. **(a, b)** Gel-electrophoretic analysis of re-dissolved pellets of a 42-helix bundle after precipitation at a final concentration of 5-9 % PEG using only divalent $MgCl_2$ in the folding and precipitation buffer (20 mM); **(c, d)** Gel-electrophoretic analysis of a reaction mixture of a 42-helix bundle that was self-assembled using only monovalent NaCl in the folding and precipitation buffers (2 M). The samples were analyzed after precipitation at a final concentration of 5-9 % PEG and 2 M NaCl; **(e, f)** Gel-electrophoretic analysis of re-dissolved pellets of a 42-helix bundle prepared by using default precipitation buffer (containing both monovalent and divalent ions) after incubation of the mixture of sample and PEG solution at 0 °C and RT. The upper row depicts dissolved pellets (a, c, e); the bottom row of images depicts corresponding supernatants (b, d, f).

Screen of salt concentrations

Variations of salt concentrations in presence of both monovalent and divalent cations suggested that requirements for lower concentration of one type of cation can be partially compensated by a higher content of PEG or the other salt component (Figure S5). In presence of 255 mM NaCl in the mixture of sample and PEG precipitation buffer, a final concentration of 10 mM $MgCl_2$ was best for optimal recovery of DNA objects (Figure S5a,b). At 10 mM $MgCl_2$ in the mixture of sample and PEG solution, concentrations of 250 mM NaCl or higher lead to better sample recovery (Figure S5c,d). In general, higher salt concentrations lead to increased fractions of residual staple strands in the purified samples (visible when increasing the brightness of Figure S5a, c). Missing samples in lane 19 in (a) and lane 5 in (c) were caused by accidental loss of the pellet at the wall of the pipet tip during removal of the supernatant.

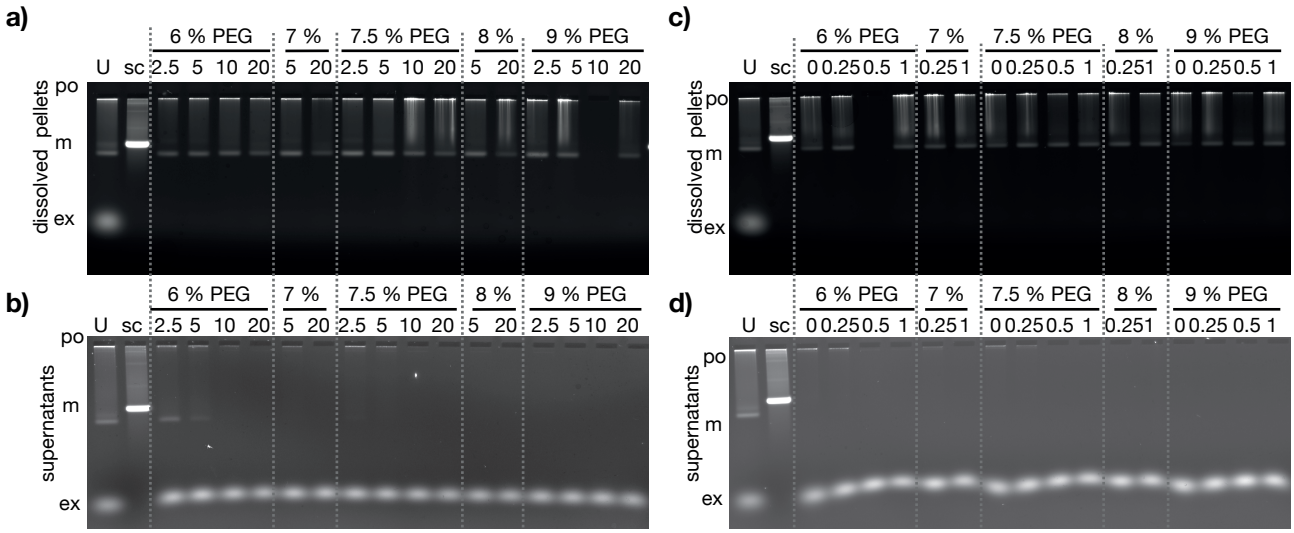

Figure S5. Screen of salt - and PEG concentrations in presence of sodium and magnesium ions. Images showing gel-electrophoretic analysis of dissolved pellets **(a, c)** and corresponding supernatants **(b, d**) of PEG purified 42-helix bundle. **a, b)** constant concentration of 255 mM NaCl and varying concentrations of PEG (% w/v) and $MgCl_2$ (mM) **c, d)** constant concentration of 10 mM $MgCl_2$ and varying concentrations of PEG (% w/v) and NaCl (M) in the mixture of sample and PEG solution. **Labels:** U: unpurified sample; sc: scaffold strands only; po*:* gel pocket; m: monomer band of folded particles; ex: non-integrated staple strands.

Gel-electrophoretic mobility of PEG purified samples

We tested the gel-electrophoretic mobility of re-dissolved pellets after different incubation times in the buffer that was added to the pellet. After overnight-incubation, a purified sample of the 42-helix bundle exhibited identical band patterns as the unpurified sample, while re-dissolved samples that were analyzed directly after dissolving the pellet (that is, adding the buffer and mixing) exhibited a band pattern that featured a trailing smear after the leading band (Figure S6a). Nonetheless, our experiments suggest that the overall concentration of particles is not affected if a re-dissolved sample is immediately used after dissolving the pellet for further treatment, as shown in Figure 3a, where an incubation time of approx. 30 min between every cycle of PEG treatment was sufficient to re-establish an equilibrated distribution of particles.

As discussed in the main text, some objects featured an enhanced electrophoretic mobility after stripping off excess staples strands using PEG precipitation. However, when adding staple strands again to a PEG purified sample, the original electrophoretic mobility can be reconciled (Figure 2b, Figure S6b).

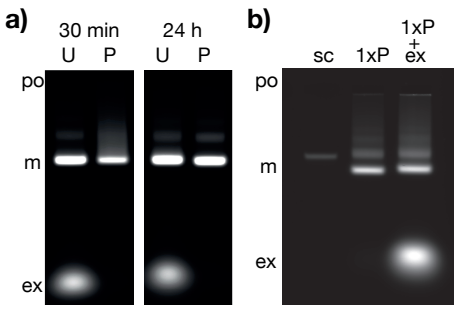

Figure S6. Reference controls with respect to incubation time and migration distance. **a)** Image of a gel showing electrophoretic analysis of a 42-helix bundle that was incubated for 30 min (left) and 24 hours (right) at room temperature after re-dissolving the pellet. **b)** Image of a gel showing electrophoretic analysis of the migration behavior of a PEG-purified sample of the 42-helix bundle in pre- and absence of excess of non-integrated staple strands. **Labels:** U: unpurified reaction mixture; sc: scaffold strands only; po: gel pocket; m: monomer band of folded particles; ex: non-integrated staple strands; 1xP: once-PEG purified sample; 1xP+ex: addition of 150 nM excess staple strands to a once-PEG purified sample.

Note S4: Complete removal of residual PEG

To test to which extent residual PEG molecules can be removed from samples that were treated with our PEG precipitation method, we purified a reaction mixture of the 42-helix bundle with a PEG solution that contained a 1 to 5 mixture of FITC-labeled PEG 8000 (fPEG) versus unlabeled PEG 8000. We subjected the purified and re-dissolved samples to three cycles of filtration using devices with different molecular weight cut-off membranes of 10 kDa, 30 kDa and 100 kDa and analyzed all samples by gel-electrophoretic separation. We quantified residual fPEG by individual detection of the fluorescein-signal and demonstrated that all three filtration devices were efficient in removing the fraction of fPEG molecules that migrated into the gel after three cycles of filtration ("fPEG" in Figure S7 a,c). Filtration devices are apparently more efficient in removing the 8 kDa-sized PEG molecules as opposed to removing non-integrated staple strands, since two more cycles of filtration were necessary to reach almost complete removal of non-integrated 16 kDa-sized staple strands (Figure 2d-f, (Langecker, Arnault et al. 2012)). We recovered 60 % and 65 % of the original sample after PEG purification followed by three washing cycles with 10 kDa and 30 kDa filtration devices. Filtration with 100 kDa filters resulted in a lower recovery of 48 % after three cycles of filtration. The combination of PEG purification with low-molecular weight cut-off filtration appears an ideal combination to prepare pure solutions of DNA origami objects at arbitrary object concentration and with no residual PEG contamination.

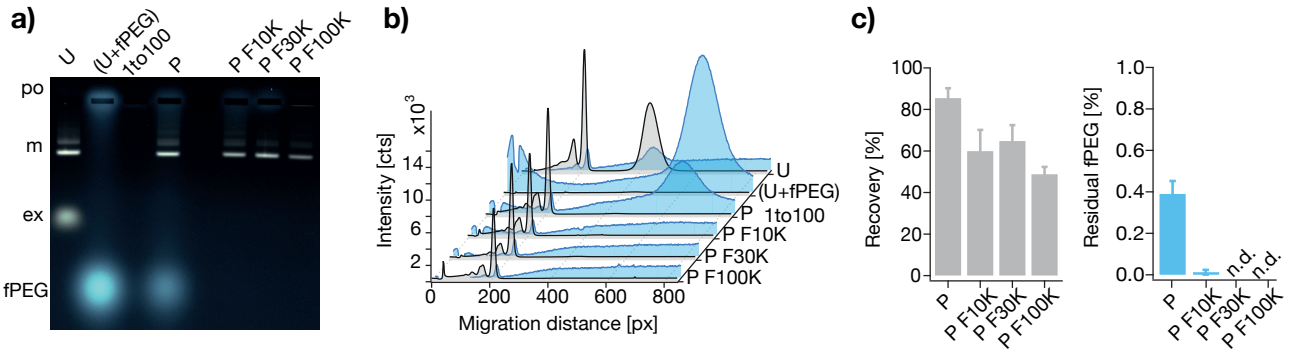

Figure S7. Agarose-gel-electrophoretic analysis for estimation of the removal of residual PEG by filtration. **a)** Overlay image of two scans of the same gel, recorded separately for the ethidium bromide (grayscale) and fluorescein (blue) emission channels. Samples were taken before (U) and after (U+fPEG) addition of precipitation buffer and compared to the re-dissolved pellet (P) of the precipitation and to samples that were further filtrated using filter devices with a 10 kDa (P F10K), 30 kDa (P F30K), or 100k Da (P F100K) molecular weight cutoff membrane. The U+fPEG sample was diluted 1 to 100 in default buffer to achieve comparable signal strength for quantification. **b)** Cross-sectional lane profiles from ethidium bromide channel (gray) and fluorescein channel (blue). **c)** Recovery of folded objects (left) relative to unpurified reaction mixture and of residual fluorescein-PEG (right) relative to the U+fPEG sample, as determined by integrating the areas of the peaks reflecting folded objects and fPEG, respectively. The experiment was performed in

triplicate, each experiment gave consistent data as in (a). Error bars in (c) indicate the standard deviation in the recovery and residuals, respectively. Labels: po: gel loading pocket; m: folded objects; ex: non-integrated excess staple strands; fPEG: fluorescein-labeled PEG.

During gel-electrophoresis, fluorescein-PEG typically migrates towards the anode, which is due to a negative charge contribution of two FITC-labels per molecule. As expected, the migration speed of the the fPEG-polymer with a size range of 7-9 kDa is faster than non-integrated staple strands with an average size of 16 kDa. Noteworthy, gel electrophoretic analysis also revealed that the labeled fPEG solution also contained a small fraction of material that did not enter the gel (Figure S7a, b). We speculate that this material could be associated with an uncharged fPEG fraction, a fraction with higher molecular weight, or with insoluble material that we also observed in the stock solution of fPEG. We estimate the size-range of the higher molecular fPEG species to 30 - 90 kDa, since complete removal of this higher molecular fraction could only be achieved using 100 kDa cut-off membranes for filtration, as shown in the detected lane profiles at migration distances from 0 to 200 px (Figure S7b). It is possible that this high molecular weight fraction is a particularity of fluorescein labeled PEG molecules and thus may not necessarily present in unlabeled PEG 8000 solutions with an average size range of 7.3 - 9 kDa, as indicated by the supplier (Carl Roth).

Note S5: Preparation of solid material containing DNA objects

Drying and re-dissolving single-layer objects

To demonstrate that drying of PEG precipitated samples is also applicable to single-layer DNA origami objects, we prepared a 20 ml scale folding reaction mixture for a variant of Paul Rothemund's single-layer DNA rectangle. The self-assembly reaction products were subjected to our PEG precipitation protocol and then dried as described in the manuscript for the multi-layer objects in Figure 3. We obtained approximately 6 mg of solid grayish-white material containing the unlabeled single-layer DNA object (Figure S8) which we subsequently re-dissolved. TEM micrographs and gel-electrophoretic analysis of the re-dissolved samples revealed well-folded particles (Figure S8 b, c). Average single particle micrographs (Figure S8c insets) of dried (left) and non-dried (right) particles confirm in greater detail that single-layer objects do survive the drying procedure without taking any apparent damage.

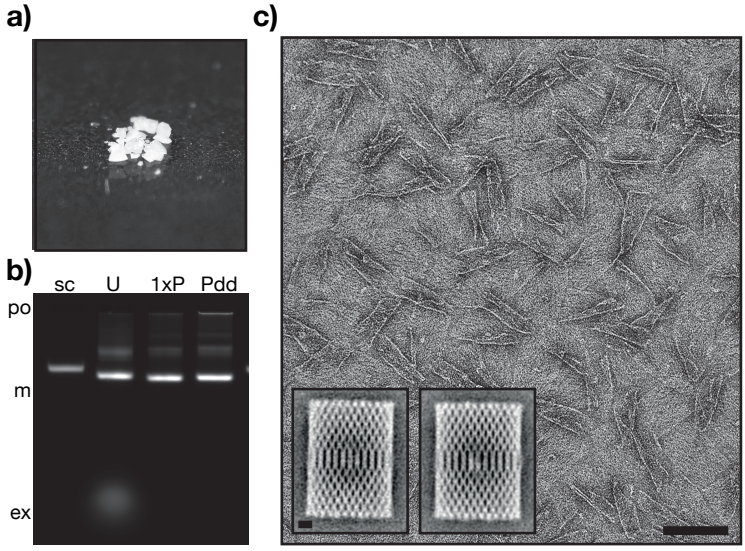

Figure S8. Preparation of solid material and dense solutions containing intact single-layer DNA objects. **a)** Approx. 6 mg of solid material containing a variant of Rothemund's Rectangle. **b)** Gel-electrophoretic analysis of an untreated reaction mixture in comparison to a once-PEG precipitated sample and a sample that was PEG precipitated, dried and re-dissolved in default buffer. **Labels:** sc: reference sample consisting of scaffold strands only; U: unpurified reaction mixture; po*:* gel pocket; m: monomer band of folded particles; ex: non-integrated staple strands; 1xP: once-PEG purified sample; Pdd*:* twice-PEG precipitated, dried and re-dissolved sample. **c)** TEM micrographs of dried and re-dissolved variant of Rothemund's Rectangle. The rolled-up / twisted appearance is expected by design. Insets: average single-particle micrographs obtained from non-dried (left) and dried and re-dissolved samples (right); scale bars: 100 nm (field-of-view micrographs), 10 nm (insets).

Drying and re-dissolving multi-layer objects

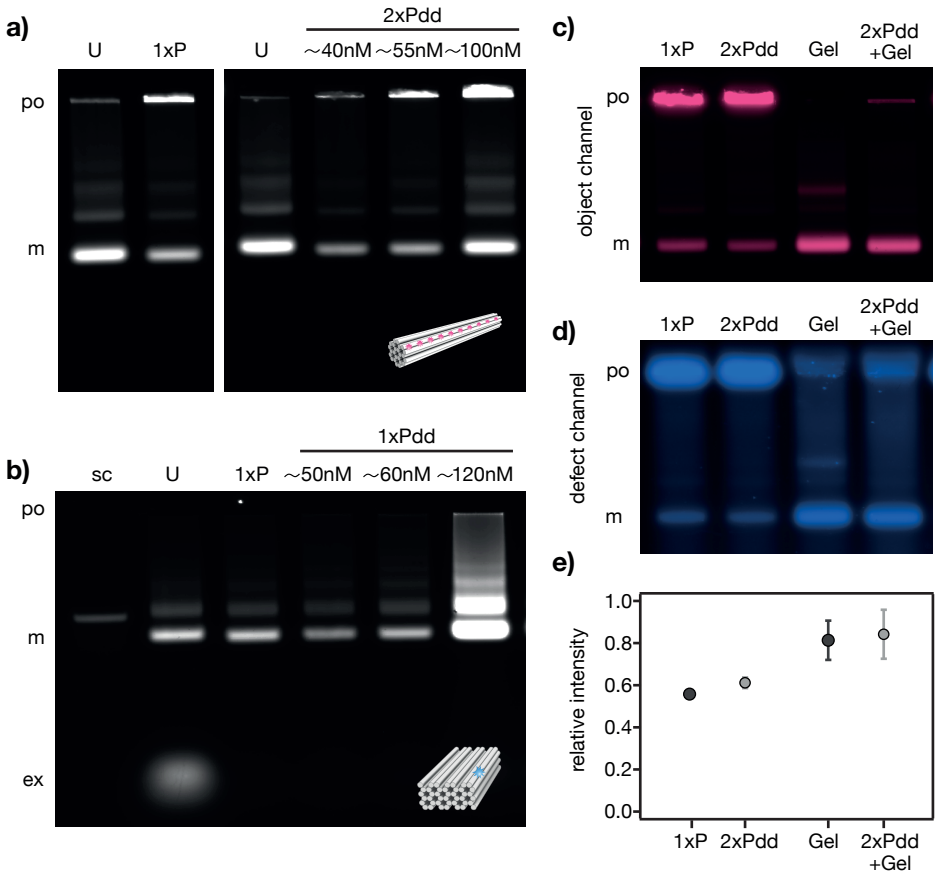

Figure S9. Structural integrity of dried and re-dissolved samples of multilayer DNA objects. Gel-electrophoretic analysis of an untreated reaction mixture in comparison to a once-PEG precipitated sample and a sample that was PEG precipitated, dried and re-dissolved in default buffer: **(a)** 24-helix bundle; **(b)** 42-helix bundle. The dense solutions were diluted for the purpose of electrophoretic analysis, the indicated concentrations were estimated from the dilution factor and the measured concentration of of particles in a 1 to 100 dilution. **(c-e)** Defect analysis of dried and redissolved 24-helix bundle in comparison to non-dried 24-helix bundle. Defect probes were analyzed in a stain-free 3 % agarose gel that was laser-scanned in the object-specific **(c)** cyanine-3 fluorescence emission channel and for the defect-specific **(d)** cyanine-5 fluorescence emission channel; **(e)** relative intensity was calculated as the ratio of peak intensities of the co-localized folded object bands as seen in the cy5 versus cy3 emission channel. **Labels:** po*:* gel pocket; m: monomer band of folded particles; ex: non-integrated staple strands; sc: reference sample consisting of scaffold strands only; U*:* unpurified reaction mixture; 1xP: once-PEG purified sample; 1xPdd/2xPdd: once or twice-PEG precipitated, dried and re-dissolved sample; 2xPdd + Gel: a sample of 2xPdd that was subjected to AGE-purification; Gel: untreated reaction mixture that was purified using AGE.

Estimation of DNA mass in the solid material

To quantify the amount of DNA when we re-dissolved the dried samples in buffer, we used absorption measurements assuming an extinction coefficient of 0.02 µg ml^{-1} cm^{-1} (standard value for double-stranded DNA). These measurements indicated a total DNA mass of 3.2 mg for the re-dissolved Rothemund rectangle sample, 3.3 mg for the re-dissolved 42-helix bundle sample, and 4.2 mg for the re-dissolved 24-helix bundle sample.

Assuming 100 % folding yield, 20 ml of such an reaction at a concentration of 50 nM template single-strand can give at maximum 1 nanomole of folded DNA objects. Regarding the fact that 2 ml sample were extracted for final comparison of sample quality, the expectable total mass of DNA in the obtained solid material was 4.5 mg in all three samples (Rothemund rectangle, 42-helix bundle, 24-helix bundle). However, material losses were incurred in particular when we transferred the solid material for documentation purposes from the pelleting tube to a watch-glass and back (see photos in Figure 3 a-c). At both steps we observed small crumps that irreversibly got stuck to the walls of both receptacles. We thus attribute the discrepancies between masses determined by absorption measurements and expectation to these losses.

The values obtained by absorption spectroscopy may be contrasted with the absolute mass of dry material that we obtained which were 6.8 mg for the Rothemund rectangle sample, 5.5 mg for the 42-helix bundle, and 8.4 mg for the 24 helix bundle. Hence, approximately 50% of the measured dry weight actually account for DNA mass. We attribute the remaining 50% to residual PEG, H_20 and salt molecules.

Note S6: Supplementary References

Scheres, S. H., R. Nunez-Ramirez, C. O. Sorzano, J. M. Carazo and R. Marabini (2008). "Image processing for electron microscopy single-particle analysis using XMIPP." Nat Protoc **3**(6): 977-990.

Tang, G., L. Peng, P. R. Baldwin, D. S. Mann, W. Jiang, I. Rees and S. J. Ludtke (2007). "EMAN2: an extensible image processing suite for electron microscopy." J Struct Biol **157**(1): 38-46.

Wagenbauer, K. F., C. H. Wachauf and H. Dietz (2014). "Quantifying quality in DNA self-assembly." Nat Commun **5**: 3691.

Bai, X.-C., Martin, T.G, Scheres, S.J., and Dietz, H. (2012). “Cryo-EM structure of a 3D DNA-origami object.” Proc Natl Acad Sci USA **109**: 20012-20017.

Langecker, M., V. Arnaut, T. G. Martin, J. List, S. Renner, M. Mayer, H. Dietz, F. C. Simmel (2012). “Synthetic lipid membrane channels formed by designed DNA nanostructures.” Science **338**(6): 932–936.

Bellot, G. et al., (2013). DNA nanotubes for NMR structure determination of membrane proteins. Nature Protocols **8**(4): 755–770.

Humphreys, G.O., Willshaw, G.A. & Anderson, E.S., (1975). A simple method for the preparation of large quantities of pure plasmid DNA. Biochimica et biophysica acta **383**(4): 457–463.

Sambrook, J., Russell, D.W. & Irwin, N., (2001). *Molecular cloning : a laboratory manual*, Cold Spring Harbor, NY: Cold Spring Harbor Laboratory Press.

Stein, V. et al., (2009). An efficient method to assemble linear DNA templates for in vitro screening and selection systems. Nucleic Acids Research **37**(18): e122–e122.

Vajda, B.P., (1978). Concentration and purification of viruses and bacteriophages with polyethylene glycol. Folia microbiologica **23**(1): 88–96.

Yamamoto, K.R. et al., (1970). Rapid bacteriophage sedimentation in the presence of polyethylene glycol and its application to large-scale virus purification. Virology **40**(3): 734–744.

Zimmerman, S.B. & Minton, A.P., (1993). Macromolecular crowding: biochemical, biophysical, and physiological consequences. Annu Rev Biophys Biomol Struct **22**: 27-65.